A98-31504 ICAS-98-2,4,3

SELF-EXCITED OSCILLATIONS OF SUPERSONIC OPPOSING JET FLOW

Masahiro Fujita
Staff Researcher
Mitsubishi Research Institute, Inc.
Chiyoda, Tokyo, Japan

Keiichi Karashima
Professor
Nishinippon Institute of Technology
Miyako, Fukuoka, Japan

Abstract

The purpose of the present study is to validate quantitatively the theoretical models suggested in the previous study of one of the authors, in which the mechanism of self-excited oscillations of a supersonic opposing jet flow in a supersonic free stream was interpreted physically. Wind tunnel experiments as well as computations are conducted to obtain unsteady flow fields at several total pressure ratios of jet to free stream. The Mach number of free stream and jet are 2.5 and 1.5, respectively. In the experiment, a hemisphere-cylinder model with a jet nozzle at its stagnation point is employed, and unsteady surface pressure is measured by pressure-transducers which are directly embedded into the model. In the computation, a time-accurate algorithm using a viscous compressible flow model is applied to the identical configuration as the experimental model. Unsteady solutions are obtained by a finite difference method which consists of high-resolution upwind space differencing and second-order explicit time integration. The results obtained show that the frequency of oscillations depends on the total pressure ratio and the scale of model examined. The numerical solutions compare well with the experimental results, and the theoretical models mentioned above have been validated quantitatively.

Nomenclature

c Sound speed
d Jet exit diameter
e Total energy per unit volume
J Transformation Jacobian
p Pressure
Pr Prandtl number for air
Re Reynolds number based on the body diameter and the free stream condition
r Spatial coordinate normal to the body axis
t Nondimensional time based on the body diameter and the free stream sound speed
U Contravarient velocity component along the ξ axis
u Velocity component along the x axis
V Contravarient velocity component along the η axis
v Velocity component along the r axis
x Spatial coordinate along the body axis
γ Specific heat ratio
ϕ Angle from stagnation point along the body surface
η Transformed coordinate normal to the body
μ Viscosity coefficient
ξ Transformed coordinate along the body
ρ Density

Superscript:
n Evaluated at time $n\Delta t$
$'$ Evaluated behind the bow shock

Subscript:
j Values of the opposing jet
∞ Evaluated in the free stream
0 Stagnation values

Background

The opposing jet problem has attracted many researchers for a long time not only because of the good applications but also of the physical complexity.[1),(2)] The oscillation of the flow field observed in some conditions of the jet has been one of the most interesting problems. It has been clarified

21st ICAS Congress
13-18 September 1998
Melbourne, Australia

in previous studies that the primary parameter which affects the flow field is the ratio of jet total pressure to free stream total pressure.[3]-[5] When the total pressure ratio is more than a critical value, the flow field is almost stable and a Mach disk can be clearly observed inside the jet (denoted as *stable flow*). When the total pressure ratio is under this value, the flow field becomes unstable and the bow shock oscillates intensely (denoted as *unstable flow*). The critical value of the total pressure ratio depends on a free stream Mach number and a jet exit Mach number. Near the critical value, the flow field results in either stable or unstable flow and it tends to alter from one to another in turn (denoted as *transition*).

Time averaged flow field

One of the authors has investigated the oscillatory opposing jet flow by a method of computation.[6],[7] In that study, five total pressure ratios of jet to free stream were examined to obtain the stable, unstable and transitional flow. The variation of the time-averaged body surface pressure at 15 degrees position measured from the symmetric axis have been examined. This position is located in the recirculating region described below in every cases. An abrupt rise of the surface pressure at a certain total pressure ratio corresponded to the transition from an unstable flow to a stable flow. The computed and experimental pressure curves agreed qualitatively. The transition occurred at nearly the same total pressure ratio both in the computation and in the experiment.

A series of numerical solution obtained at each time step was averaged in time for comparison with the experiment. Comparing with the schlieren photograph, it could be said that the shapes and locations of the bow shock and the Mach disk for the stable flow agreed well with each other. The time-averaged density contours for the unstable flow was illustrated. Contrary to the stable flow case, contours of the bow shock and the Mach disk were obscured, which seemed to agree with the schlieren photograph. This might suggest that the bow shock and Mach disk oscillated at a considerably large amplitude, and the period of oscillation was much shorter than the exposure time. Comparisons of the surface pressure distribution between the time-averaged numerical solutions and the experimental data were also carried out. Considerable decrease in pressure around the jet occurred as a result of a large separation of the jet flow. In both stable and unstable cases, pressure curves obtained from the computation agreed fairly well with the experimental data.

As a result of these comparisons, it was shown that many features of the opposing jet flow observed in the experiments, such as the existence of stable and unstable flow, the transition between them, can be explained through the numerical solution. Therefore, the accuracy of the simplified flow model used under the assumption of the axisymmetric flow could be considered as satisfactory in resolving the opposing jet flow field.

Stable flow model

Some researchers have already developed models of explaining stable flow.[8],[9] A more precise model of explaining stable flow has been suggested in the previous study by one of the authors on basis of the result of computations.[6],[7] Figure 1 shows the stable flow model suggested. Although this model is roughly similar to that of other researchers, special attention is paid to the structure of the jet. It is illustrated that the supersonic flow, which passes the barrel shock and the reflected shock emanating the triple point, is finally decelerated to subsonic speed by a terminal shock. There is a subsonic pocket around the symmetrical axis bounded by the bow shock, the Mach disk and the terminal shock. The fluid, which is nearly still in the subsonic pocket, begins to flow downstream along the jet boundary

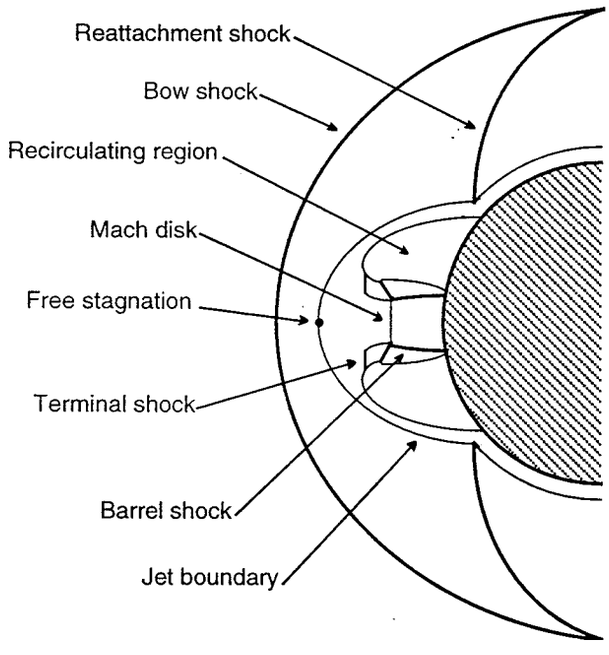

FIGURE 1 - Stable flow model

and is accelerated again to supersonic speed.

The existence of a slight unsteadiness has also been reported even for the stable flow case.[6] Although the entire flow field is expected to be nearly stable, the numerical solution oscillated about its neutral position in an amplitude less than the width of the thick line representing a bow shock in the photograph. An oscillation with an amplitude this small cannot be found in a normal schlieren photograph. Thus, this oscillatory solution may correspond to the small oscillation described in previous studies.

Unstable flow model

Contrary to the stable flow case, the computed flow field exhibited a nearly periodic oscillation with large amplitude. The distance between the stagnation point and the bow shock, measured along the symmetrical axis, reached up to a few times as that of the no jet case, and its amplitude was about 10 ~ 20 % of the body diameter. Although there are no quantitative experimental data to confirm that solution, it appears that this represented the oscillatory flow observed in the wind tunnel experiments.

For the unstable flow case, the drastic change of the jet structure was illustrated in a time series of instantaneous flow fields. The sequence of the flow field started from the stage when the jet length was shortest in the period of oscillation. At this moment, the supersonic jet terminated through a nearly normal shock (Mach disk), and immediately lost its total pressure down to the value of the free stagnation. The structure of the first cell of the jet changed with time to the regular reflection type, and the second cell of the jet appeared following the first cell. As a result, the jet length gradually increased so that both the bow shock and the free stagnation also moved away from the body, although the position of the free stagnation was not discernible. At this phase, the jet flow experienced a pair of oblique shocks in the first cell, until being terminated by a normal shock in the second cell, after which a longer distance was required to lose its total pressure completely down to the value of the free stagnation.

An abrupt transition of the shock structure in the first cell occurred, when the regular reflection of the barrel shocks changed to the Mach reflection. This was followed by the increase in the diameter of the Mach disk, when the entire flow after the Mach disk becomes subsonic, so that the Mach disk at the end of the second cell disappeared. The disappearance of the Mach disk in the second cell meant the breakdown of the second cell. Subsequently, the jet length was suddenly shortened, so that the bow shock and the free stagnation also began to move back toward the body. Consequently, the length of the first jet cell returned to the original value at the end of the period, and a shape of the jet was nearly identical to the original one.

Love et al.[10] made a detailed experimental and theoretical study of axisymmetric free jets. Their most important finding was that in a sonic jet case, the jet structure changed from the Mach reflection type to the regular reflection type, when the surrounding pressure is more than 1/2 of the jet exit pressure. On the basis of the above finding on a free jet, a model of the oscillation for the unstable flow was developed as shown in Figure 2.

At the beginning of the cycle in Figure 2(a), where the bow shock is at the most backward position in the period of oscillation and the volume of recirculating region is at the minimum, there is only one jet cell, which contains a normal shock at the end. At this time, the pressure in the recirculating region, i.e. the pressure surrounding jet, gives the maximum value which is more than the threshold value of the change of jet structure, as shown in Figure 2(b). Consequently, the structure of first jet cell rapidly changes to the regular reflection type which is generally called *slightly under-expanded jet*, whereby a second cell appears ahead of the first cell, as shown in Figure 2(c). This means that the length of the jet, defined as the distance from the jet exit to the

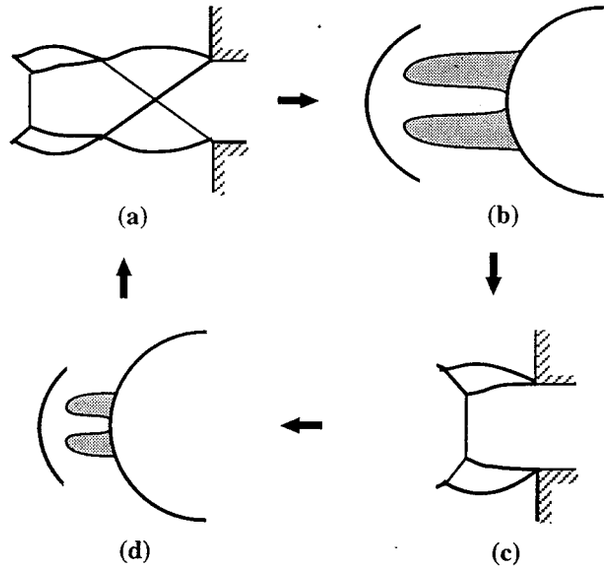

FIGURE 2 - Oscillatory flow model

free stagnation, increases with time. The length of the jet is at the maximum value when the free stagnation point reaches its most forward position. In this phase, the long jet including two cells increases the volume of the recirculating region, reducing its pressure. As a result, the pressure surrounding the jet may become less than the threshold value of the change of the jet structure, and the structure of the first cell changes to the Mach reflection type which is called *highly under-expanded jet* as shown in Figure 2(d). After this change, the flow passing the Mach disk in the first cell becomes subsonic, which causes the second cell to disappear instantly. The free stagnation now rapidly moves backward, i.e. the length of the jet decreases with time. Finally the length of the jet gives its minimum value again, at which time the volume of the recirculating region is also at its minimum, as shown in Figure 2(a). The change of the flow field repeats in this cycle.

Transition model

Finley[8] has suggested the condition of transition between the stable and unstable flow by a theoretical analysis. According to Finley, the transition occurs at the total pressure ratio at which the location of the jet terminal shock coincides with that of the first intersection of barrel shocks in a jet cell. The location of the jet terminal shock satisfies the static condition of the opposing jet. On the other hand, the location of the first intersection of barrel shocks coincides with that of an equivalent free jet, whose surrounding pressure is equal to the pressure in the recirculating region. The condition of Finley was validated quantitatively, on the basis of the previous numerical results[6],[7]. In order to discuss Finley's condition, it is necessary to obtain the location of the Mach disk and the shock intersection on the axis as a function of the total pressure ratio. The distance from jet exit to the Mach disk which is required to attain the static condition has been calculated by Romeo[11], using the formula of Ashkenas and Sherman[12] which expresses the total pressure distribution along the center line of a sonic free jet. Furthermore, Love et al.[10] have measured the location of the first intersection of barrel shocks on the axis as a function of a ratio of the jet exit pressure to the surrounding pressure. In the case of opposing jet flow, it was necessary to use the value of computed pressure in the recirculating region as that of the surrounding pressure.

According to the time-history of the pressure in the recirculating region, the pressure tended to oscillate considerably with time for both stable and unstable flow cases. In the stable flow case, the amplitude of each oscillation of the surrounding pressure was nearly constant, and no abrupt peak exists. On the other hand, in the unstable flow case, steep peaks of the pressure could be observed which were due to the impingement of the broken jet flow on the body surface. There were the threshold which indicated transition of the shock reflection in the first jet cell, under which the Mach reflection existed while over which the regular reflection appeared. In the stable flow case, the surrounding pressure was under the threshold throughout the period, i.e. only the Mach reflection appeared. This corresponded well with the observations of the computed density contours. To the contrary, in the unstable flow case, the surrounding pressure occasionally exceeded the threshold, so that both types of reflection appear in a single period. It was noted that the surrounding pressure oscillated intensely in both cases, thus time averaged values were employed for the present estimation.

According to the variation of the location of the shock intersection with total pressure ratio, the curve which represents the location of the Mach disk could be drawn. The location of the intersecting shock coincided with that of the Mach disk at certain total pressure ratio. Above this value, the distance from the stagnation point to the intersecting shock was larger than that to Mach disk, so that the incoming flow to the Mach disk was not disturbed by any shock waves. On the other hand, under the value, the barrel shocks intersected with each other on the axis before the Mach disk, so that the expanding flow terminated at the intersecting point. As a result, a second jet cell appeared before the terminal Mach disk. If Finley's condition was applied, it was anticipated that the flow field became stable above the critical total pressure ratio. This prediction agreed quite well with the computation as well as the experimental result. Therefore it was satisfactory to say that Finley's condition was quantitatively validated.

Objectives of present study

Former researchers mainly intended to clarify the structure of the stable flow and made no detailed analysis on the unstable flow and the transition.[8],[9],[13] It was mainly due to the difficulties in the measurement of time-variation of flow characteristics, such as bow shock or pressure on the body surface, in the conventional wind tunnel

experiments. The previous study by one of the authors was successful to open a new path in the research of oscillatory opposing jet flow by use of a method of computation. The quantitative validation of the flow models suggested, however, has not been carried out. The present study attempts to validate quantitatively the flow models developed in the previous study by use of unsteady experiments and computations. The present unsteady measurement is conducted by use of a quickly responsive pressure-transducer and a memory recorder which are able to resolve time-varying phenomenon for order of nano second. The computation intends not to simulate the real flow field, but to solve the simplified equations of fluid on condition that they preserve essential properties of the flow, in order to obtain the primary phenomenon in the problem.

Method of experiment

The present experiment was conducted by use of a supersonic wind tunnel at The Institute of Space and Astronautical Science, Kanagawa, Japan. A schematic picture of a hemisphere-cylinder model tested is shown in Figure 3. The model has a jet-settling chamber inside and a conical nozzle of exit Mach number 1.5 is positioned on the center line of the model. Air at room temperature is introduced into the chamber, and its total pressure is controlled at certain prescribed value. On the surface of hemispherical nose, two pressure holes of diameter 1.0 mm are placed at the position of 20 and 35 degree from the stagnation point, respectively. Another scaleable model whose diameter is 35 mm is also examined in order to investigate scaleable effects on the frequency of oscillation.

Two pressure-transducers are directly embedded into the model at the pressure holes. The surface pressure was measured at 100 μs interval for 200 ms.

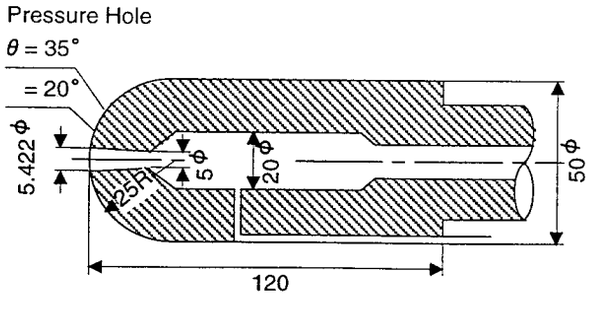

FIGURE 3 - Experimental model

Method of computation

Governing equations

It has been indicated in the previous experiments that the actual oscillating flow fields are not always axially symmetrical in spite of the employment of an axisymmetric model without an angle of attack. In the present study, however, an axisymmetric flow model is applied on the hypothesis that the essential mechanism of oscillations can be explained by the axisymmetric flow theory. This approach also allows to save computational time. The derivation of the axisymmetric form from the original three-dimensional equations has been described in appendix of the paper.[6]

In the flow field discussed here, the Reynolds number is high enough that the returning jet and recirculating flow can be considered to be fully turbulent. But the frequency of the oscillations discussed here is much lower than that of usual turbulent fluctuations of free jets[14]-[16] and it has been showed by previous investigations of the free jet that the jet boundary in the vicinity of the jet exit remains laminar.[17] Thus it is assumed that the turbulence effect does not directly affect the oscillations of the flow field. Under the above assumptions, no turbulent model will be used here.

In the previous study, a sub grid for the jet nozzle was included in order to give the emanating jet condition more accurately. [7] That is, the jet condition was imposed on the jet inlet in the sub grid as the jet chamber condition, and flow in the jet nozzle had been solved as well as the flow field around the body. The result showed, however, no significant deference from more simple case in which the uniform jet flow was specified as the boundary condition at the jet exit. Therefore, in the present computation, flow in the jet nozzle is not be solved and simplified jet boundary condition above has been applied.

The non-dimensionalized axisymmetric Navier-Stokes equations transformed to general curvilinear coordinates are

$$\frac{\partial \hat{Q}}{\partial t}+\frac{\partial \hat{F}}{\partial \xi}+\frac{\partial \hat{F}}{\partial \eta}+\hat{H}=\frac{1}{Re}\left(\frac{\partial \hat{F}_v}{\partial \xi}+\frac{\partial \hat{F}_v}{\partial \eta}+\hat{H}_v\right) \qquad (1)$$

Each vector in both members of the equations is expressed as

$$\hat{Q}=\frac{1}{J}\begin{pmatrix}\rho\\ \rho u\\ \rho v\\ e\end{pmatrix},\ \hat{F}=\frac{1}{J}\begin{pmatrix}\rho U\\ \rho uU+\xi_x p\\ \rho vU+\xi_r p\\ (e+p)U\end{pmatrix},$$

$$\hat{G}=\frac{1}{J}\begin{pmatrix}\rho V\\ \rho uV+\eta_x p\\ \rho vV+\eta_r p\\ (e+p)V\end{pmatrix},\ \hat{H}=\frac{1}{J}\begin{pmatrix}\rho v/r\\ \rho uv/r\\ \rho v^2/r\\ (e+p)v/r\end{pmatrix},$$

$$\hat{F}_v=\frac{1}{J}\begin{pmatrix}0\\ \xi_x\tau_{xx}+\xi_r\tau_{xr}\\ \xi_x\tau_{xr}+\xi_r\tau_{rr}\\ \xi_x\beta_x+\xi_r\beta_r\end{pmatrix},\ \hat{G}_v=\frac{1}{J}\begin{pmatrix}0\\ \eta_x\tau_{xx}+\eta_r\tau_{xr}\\ \eta_x\tau_{xr}+\eta_r\tau_{rr}\\ \eta_x\beta_x+\eta_r\beta_r\end{pmatrix},$$

$$\hat{H}_v=\frac{1}{J}\begin{pmatrix}0\\ \tau_{xr}/r\\ \sigma/r\\ \beta_r/r\end{pmatrix}$$

The stress and heat flux terms in the viscous fluxes are expressed as

$$\tau_{xx}=\frac{1}{3}\mu\left\{4\left(\xi_x u_\xi+\eta_x u_\eta\right)-2\left(\xi_r v_\xi+\eta_r v_\eta\right)-\frac{2v}{r}\right\}$$

$$\tau_{rr}=\frac{1}{3}\mu\left\{4\left(\xi_r v_\xi+\eta_r v_\eta\right)-2\left(\xi_x u_\xi+\eta_x u_\eta\right)-\frac{2v}{r}\right\}$$

$$\tau_{xr}=\mu\left(\xi_r u_\xi+\eta_r u_\eta+\xi_x v_\xi+\eta_x v_\eta\right)$$

$$\sigma=2\mu\left(\xi_r v_\xi+\eta_r v_\eta-\frac{v}{r}\right)$$

$$\beta_x=u\tau_{xx}+v\tau_{xr}+\frac{\mu}{Pr(\gamma-1)}\left(\xi_x c^2{}_\xi+\eta_x c^2{}_\eta\right)$$

$$\beta_x=u\tau_{xr}+v\tau_{rr}+\frac{\mu}{Pr(\gamma-1)}\left(\xi_r c^2{}_\xi+\eta_r c^2{}_\eta\right)$$

For the present flow condition, the air is assumed to have constant specific heat and obey the state equation of a perfect gas. Note that the ratio of specific heat γ is set to be 1.4, the Prandtl number Pr is assumed to be 0.72 and the viscosity coefficient μ is obtained through Sutherland's formula.

Solution algorithm

These equations are solved by the finite difference method and unsteady solutions are obtained at each time step through a time marching procedure. The Lax-Wendroff type explicit TVD (Total Variation Diminishing) scheme, proposed by Yee[18], is used to solve the discretized equations. The author has applied this scheme to several problems[19],[20] to date, and obtained satisfactory results in each case. The scheme is temporally and spatially second-order accurate and is suitable for the unsteady problem like the one in this study as well as steady ones.

The original scheme developed by Yee is applied to one-dimensional systems, and it is necessary to extend it to the multidimensional scheme in order to apply to the axisymmetric Navier-Stokes equations. Preserving the original second order time accuracy, the extension can be accomplished by, for example, a Strang-type fractional step method.[21] Using this method, the governing equations are at first decomposed into three equations as

$$\frac{\partial\hat{Q}}{\partial t}+\frac{\partial\hat{F}}{\partial\xi}=\frac{1}{Re}\cdot\frac{\partial\hat{F}_v}{\partial\xi} \tag{2a}$$

$$\frac{\partial\hat{Q}}{\partial t}+\frac{\partial\hat{G}}{\partial\eta}=\frac{1}{Re}\cdot\frac{\partial\hat{G}_v}{\partial\eta} \tag{2b}$$

$$\frac{\partial\hat{Q}}{\partial t}+\hat{H}=\frac{1}{Re}\hat{H}_v \tag{2c}$$

Then the solution at the next time step is obtained as

$$\hat{Q}^{n+1}=\Delta_\xi^{h/2}\Delta_\eta^{h/2}\Delta_s^{h}\Delta_\eta^{h/2}\Delta_\xi^{h/2}\hat{Q}^n \tag{3}$$

where operators $\Delta_\xi^h, \Delta_\eta^h$ and Δ_s^h are implemented for the equation (2a), (2b) and (2c) with $h=\Delta t$, respectively. Both operators Δ_ξ^h and Δ_η^h represent the 2nd-order Lax-Wendroff explicit TVD differencing for convective terms and 2nd-order central differencing for diffusive terms. The solution algorithm is expressed as

$$\Delta_\xi^h:\quad \hat{Q}^{n+1}=\hat{Q}^n-h\left(\partial_\xi\hat{F}-\frac{1}{Re}\partial_\xi\hat{F}_v\right)^n \tag{4}$$

$$\Delta_\eta^h:\quad \hat{Q}^{n+1}=\hat{Q}^n-h\left(\partial_\eta\hat{G}-\frac{1}{Re}\partial_\eta\hat{G}_v\right)^n \tag{5}$$

The operator Δ_s^h, on the other hand, denotes a 2nd-order Runge-Kutta method for both convective and diffusive source terms as follows:

$$\Delta_s^h: \quad \hat{Q}^* = \hat{Q}^n - h\left(\hat{H} - \frac{1}{Re}\hat{H}_v\right)$$
$$\hat{Q}^{n+1} = \frac{1}{2}\left\{\hat{Q}^n + \hat{Q}^* - h\left(\hat{H} - \frac{1}{Re}\hat{H}_v\right)^*\right\} \tag{6}$$

Computational grid

The domain of interest is limited to the region that is bounded by the bow shock and the body. Thus the main grid including 131×131 points is placed on the body fitting curvilinear coordinates. The present computational grid is shown in Figure 4. The grid points are clustered exponentially in the η direction in the vicinity of the body surface. The minimum grid spacing at the body surface is given as 1/1000 of the body diameter. The grid points in the ξ direction are clustered in the jet exit region and the minimum spacing at the lip of the jet exit is nearly same magnitude of that at the body surface in the η direction. All solutions to be described later including the case without a jet have been obtained using the same computational grid here. The flow field was computed using coarser grids as a preliminary study. It was found from the result that using a fine grid gives the same solutions of unsteady flow as coarser grids, except slightly high resolution of shocks and shear layers. Thus it can be concluded that the present numerical solutions have converged to the mathematical solutions.

Boundary and initial conditions

The boundary conditions on each boundary of the computational domain are implemented numerically as follows: the variables on the inflow boundary are fixed to free stream values. On the outflow boundary, the variables are given by linear extrapolation from variables on the internal grid points. Those on the body surface are given by no-slip, zero-pressure-gradient and adiabatic wall conditions. On the symmetric axis, zero-order extrapolation is practical since this represents absence of flux

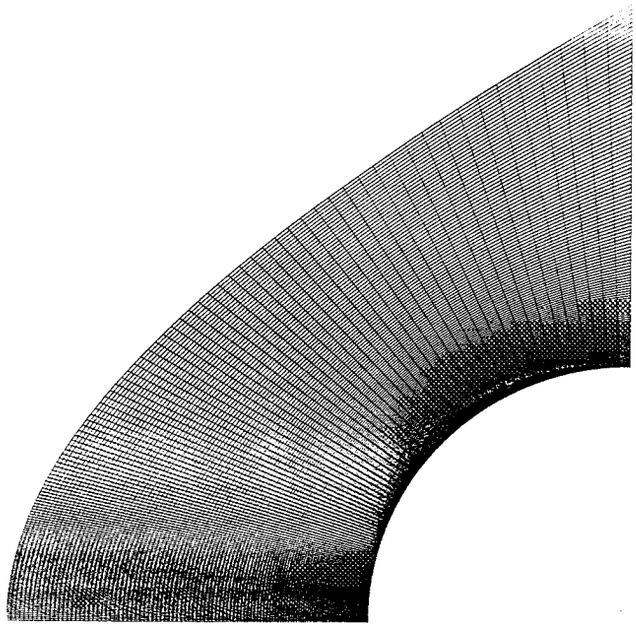

FIGURE 4 - Computational grid

condition across the axis. Finally, the values on the nozzle exit are given by use of the iso-entropy relations for the prescribed total pressure ratio and total temperature of the jet.

The initial condition corresponds to an impulsive start. Before start of calculations, the values on all inner grid points are initialized to those of a free stream.

Results and discussions

In the present study, Mach number of free stream and jet were set at 2.5 and 1.5, respectively. Total temperature of both free stream and jet was 290 K. Other flow conditions are shown in Table 1. The authors examined the flow fields for three total pressure ratios, two of which (0.656 and 0.990) were expected to correspond to unstable flow, and the remaining one (1.500) was expected to correspond to stable flow from results of previous studies.

Figure 5 shows power spectrums of time-varying location of bow shock derived from computational results for the 50 mm diameter model. The location of bow shock was measured on the stagnation line.

Table 1 - Flow conditions

	Total pressure ratio			Reynolds number
Experiment	0.654~0.658	0.986~0.993	1.480~1.522	$1.431\sim1.526\times10^6$
Computation	0.656	0.990	1.500	1.500×10^6

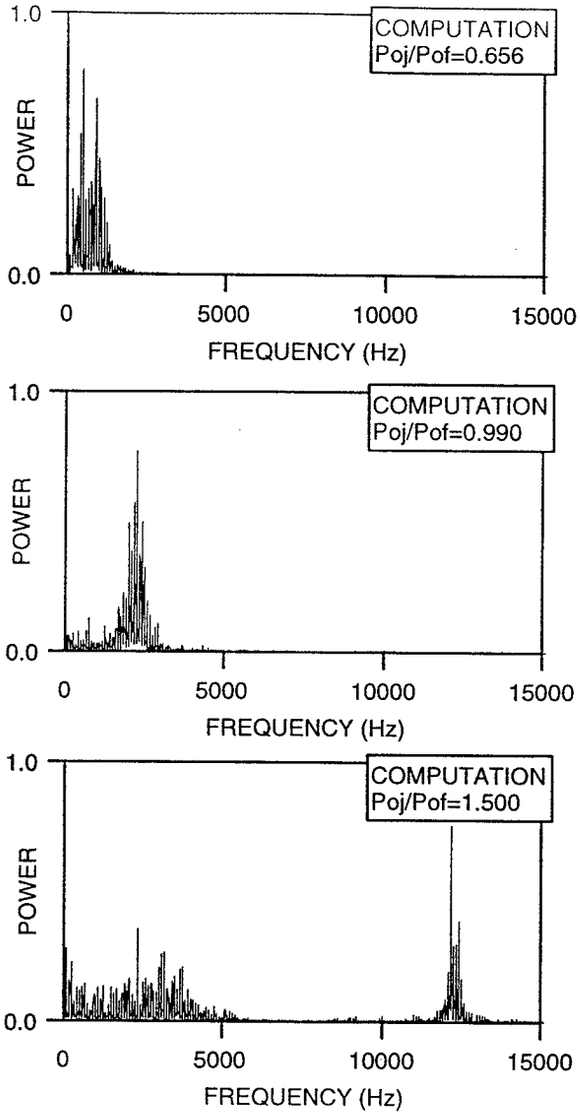

FIGURE 5 -Power spectrums of time-varying location of bow shock

In the case of total pressure ratio of 0.656, the distribution of power spectrum had several peaks at frequencies less than 1000 Hz. The frequencies of these peaks increased up to about 2000 Hz, when the total pressure ratio came to 0.990. This oscillation of bow shock represents the oscillation with large amplitude for the unstable flow described in the background section. It was found that the frequency of oscillation for unstable flow tended to increase as the total pressure ratio increased. When the total pressure ratio was 1.500, power spectrum related to oscillations for unstable flow diminished. On the other hand, another peak of power spectrum appeared at frequency more than 10 KHz. This oscillation at a higher frequency is considered to be the small oscillation for stable flow. It is clear from these figures that the present computation has been able to reproduce two types of oscillations in the opposing jet flow investigated here.

Figure 6 shows power spectrums of time varying surface pressure at the position of 35 degree on the 50 mm diameter model. It is found in the computational results that the variation of power spectrum distribution with respect to total pressure ratio is similar to that in the case of bow shock oscillation. In the case of surface pressure oscillation, however, power spectrum of more than 10 KHz appears when total pressure ratio is 0.990, and power spectrum of less than 5 KHz disappears when total pressure ratio is 1.500. Based on the difference between the oscillation of bow shock and that of surface pressure, it could be said that the two oscillations did not couple strongly with each other, and that there were different mechanisms of oscillation for stable flow and for unstable flow.

Comparison between computational and experimental results could be carried out only in a region of frequency less than 5 KHz, because of limitation of measurement in the present experiment. The computational result compared well with the experimental one in that the power spectrum of the low frequency oscillation tends to decrease as total pressure ratio increases. It is noted that in the experimental results, peak of power spectrum at frequency of about 4.5 KHz exists for all three total pressure ratios. This is independent of total pressure ratio as well as scale of model, as is illustrated in figure 7 which shows power spectrums of time-varying surface pressure for another model with diameter of 35 mm at total pressure ratio of 0.990. Therefore it is suspected that the surface pressure oscillation at 4.5 KHz is due to some fluctuations of flow in the wind tunnel or other facilities for measurement.

The effect of model scale can be investigated by comparing figure 7 with graphs in figure 6 (middle). It is found in both computational and experimental results that the spectrum peak related to low frequency oscillation tends to become higher as model scale becomes smaller, and the frequency of the spectrum peak is roughly proportional to the inverse of model diameter. Consequently, it is implied that self-excited oscillation is an unsteady phenomena characterized by Strouhal number such as Karman vortex flow.

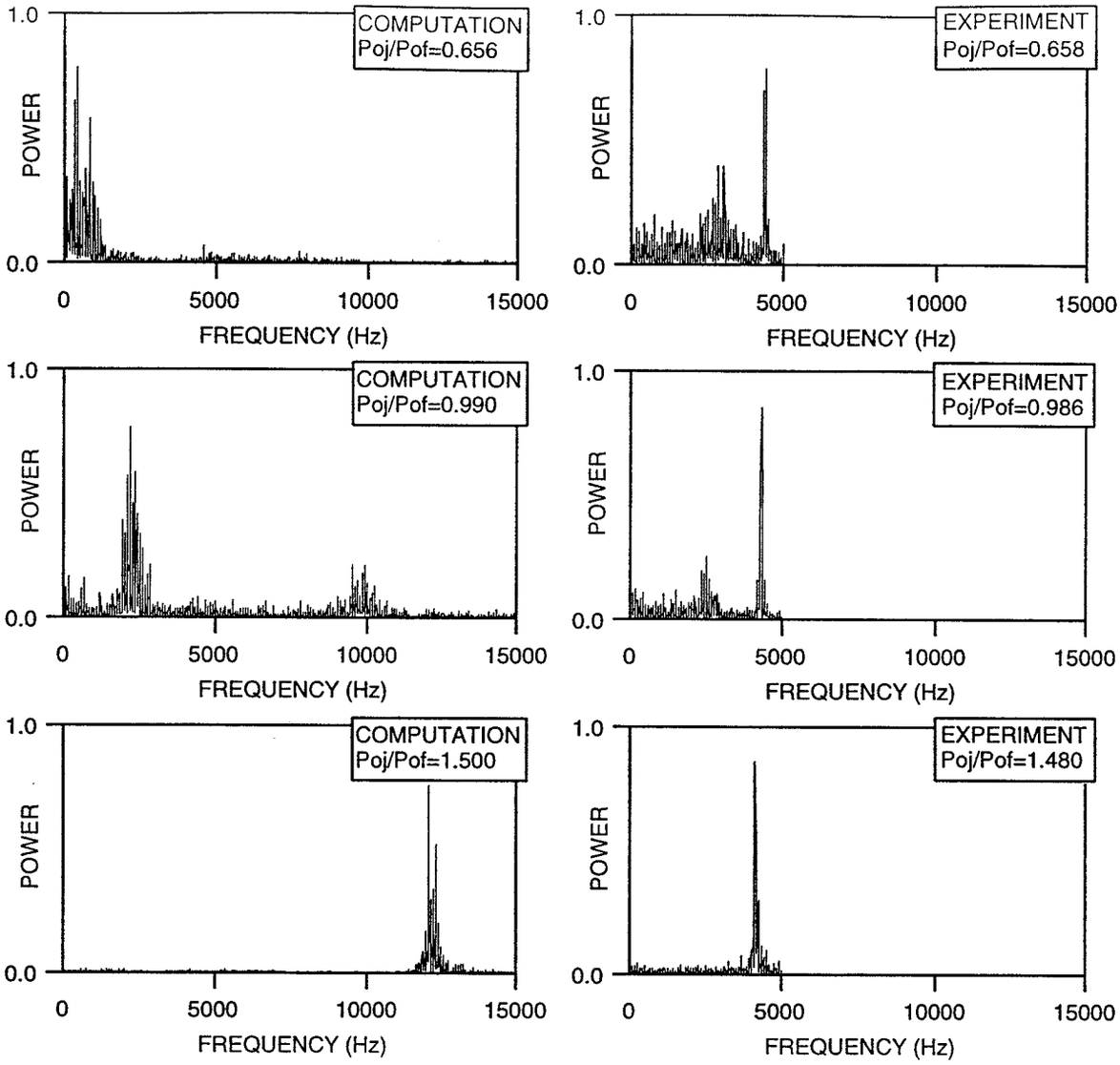

FIGURE 6 -Power spectrums of time-varying surface pressure (d=50 mm)

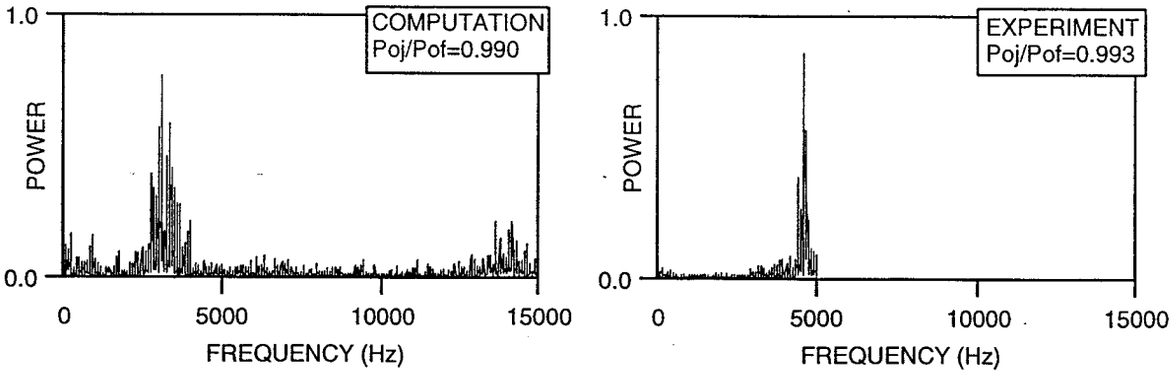

FIGURE 7 -Power spectrums of time-varying surface pressure (d=35 mm)

Concluding remarks

Unsteady computations and experiments have been applied to investigate quantitatively the self-excited oscillations of an opposing jet from a hemispherical nose. Based on the analysis of the results of experiments and computations, the following conclusions can be drawn:

- The present computation was able to reproduce two types of oscillations in the opposing jet flow.
- The oscillatory model suggested in the previous study by one of the authors has been validated quantitatively by the present experimental results
- The oscillatory flow can be characterized by Strouhal number because the frequency of oscillation is roughly proportional to the inverse of the model scale

Acknowledgments

Special thanks are due to Professor S. Aso of university of Kyushu and Mr. K. Sato of the Institute of Space and Astronautical Science for their help in carrying out the experiment.

References

(1) Warren, C. H. E., "An experimental investigation of the effect of ejecting a coolant gas at the nose of a bluff body," Journal of Fluid Mechanics, Vol. 8(part 3), 1960, pp. 400-417.

(2) Charczenko, N., and Hennessey, K. W., "Investigation of a Retrorocket Exhausting from the Nose of a Blunt Body into a Supersonic Free Stream," NASATN D-751, Sep. 1961.

(3) Hayman, L. O., Jr., "Jet Effects on Cylindrical Afterbodies Housing Sonic and Supersonic Nozzles which Exhaust against a Supersonic Stream at Angles of Attack from 90° to 180°," NASATN D-1016, Mar. 1962.

(4) Romeo, D. J., and Sterret, J. R., "Exploratory investigation of the effect of a forward facing jet on the bow shock of a blunt body in a Mach number 6 free stream," NASATN D-1605, Feb. 1963.

(5) Karashima, K., and Sato, K., "An Experimental Study of an Opposing Jet," Bulletin of Institute of Space and Astronautical Science, Vol. 11, No. 1(A), 1975, pp. 53-64.

(6) Fujita, M., "Axisymmetric Oscillations of an Opposing Jet from a Hemispherical Nose," Doctoral thesis in University of Tokyo, Mar. 1993.

(7) Fujita, M., "Axisymmetric Oscillations of an Opposing Jet from a Hemispherical Nose," AIAA Journal, Vol. 33, No. 10, 1995, pp. 1850-1856.

(8) Finley, P. J., "The flow of a jet from a body opposing a supersonic free stream," Journal of Fluid Mechanics, Vol. 26(part 2), 1966, pp. 337-368.

(9) Fox, J. H., "Counterflow Sonic Nosejet into a Supersonic Stream," AIAA paper 86-1808, 1986.

(10) Love, E. S., Grigsby, C. E., Lee, L. P., and Woodling, M. J., "Experimental and Theoretical Studies of Axisymmetric Free Jets," NASA TR R-6, 1959.

(11) Romeo, D. J., and Sterrett, J. R., "Flow Field for Sonic Jet Exhausting Counter to a Hypersonic Mainstream," AIAA Journal, Vol. 3, No. 3, 1965, pp. 544-546.

(12) Ashkenas, H., and Sherman, F. S., "The Structure and Utilization of Supersonic Free Jets in Low Density Wind Tunnels," Rarefied Gas Dynamics, edited by de Leeuw, J. H., Vol. 2, ACADEMIC PRESS, New York, 1966, pp. 84-105.

(13) Satofuka, N., and Matsuno, N., "Numerical Calculation of the Interaction between Opposing Jets and Supersonic Free Stream," Journal of Japan Society for Aeronautical and Space Sciences, Vol. 23, No. 262, 1975, pp. 586-595

(14) Powell, A., "On the Mechanism of Choked Jet Noise," The Physical Society-Section B, Vol. 66(part 12), 1953, pp. 1039-1056.

(15) Hammitt, A. G., "The Oscillation and Noise of an Overpressure Sonic Jet," Journal of the Aerospace Sciences, Vol. 28, No. 9, 1961, pp. 673-680.

(16) Tam, C. K. W., Seiner, J. M., and Yu, J. C., "Proposed Relationship between Broadband Shock Associated Noise and Screech Tones," Journal of Sound and Vibration, Vol. 110, No. 2, 1986, pp. 309-321.

(17) Kawamura, R., "Study on Axially Symmetric Supersonic Jets with Special Regard to the Shock Waves in Them," Report of Institute of Science and Technology, Vol. 6, No. 3, 1952, pp. 141-148.

(18) Yee, H. C., "A Class of High-Resolution Explicit and Implicit Shock-Capturing Methods," NASA TM 101088, Feb. 1989.

(19) Fujita, M., and Kubota, H., "Numerical Simulation of Flowfield over a Spiked Blunt-Nose," Computational Fluid Dynamics Journal, Vol. 1, No. 2, 1992, pp. 187-195.

(20) Fujita, M., and Kubota, H., "Oscillations of an Opposing Jet from a Hemispherical Nose," Proceedings of 5th International Symposium on Computational Fluid Dynamics, Sendai, Japan, 1993, pp. 215-220.

(21) Strang, G., "On the Construction and Comparison of Difference Schemes," SIAM Journal on Numerical Analysis, Vol. 5, 1968, pp. 506-517.